

Renewable hydrogen generation from a dual-circuit redox flow battery†

Cite this: *Energy Environ. Sci.*, 2014, 7, 2350

Véronique Amstutz,^a Kathryn E. Toghill,^a Francis Powlesland,^a Heron Vrubel,^b Christos Comninellis,^a Xile Hu^b and Hubert H. Girault^{*a}

Redox flow batteries (RFBs) are particularly well suited for storing the intermittent excess supply of renewable electricity, so-called “junk” electricity. Conventional RFBs are charged and discharged electrochemically, with electricity stored as chemical energy in the electrolytes. In the RFB system reported here, the electrolytes are conventionally charged but are then chemically discharged over catalytic beds in separate external circuits. The catalytic reaction of particular interest generates hydrogen gas as secondary energy storage. For demonstration, indirect water electrolysis was performed generating hydrogen and oxygen in separate catalytic reactions. The electrolyte containing V(II) was chemically discharged through proton reduction to hydrogen on a molybdenum carbide catalyst, whereas the electrolyte comprising Ce(IV) was similarly discharged in the oxidation of water to oxygen on a ruthenium dioxide catalyst. This approach is designed to complement electrochemical energy storage and may circumvent the low energy density of RFBs especially as hydrogen can be produced continuously whilst the RFB is charging.

Received 10th January 2014
Accepted 26th March 2014

DOI: 10.1039/c4ee00098f

www.rsc.org/ees

Broader context

Renewable energy technologies have evolved to deliver hundreds of terawatt hours of electricity, yet without its direct utilization in the grid part of that energy could be lost. In order to establish a thriving renewable energy economy it is of paramount importance that intermediate energy storage systems be developed. Mediating electricity production and usage will overcome the issues relating to intermittency, which presently limits widespread dependence on wind and photovoltaic power. Various approaches are under development, but no single approach is liable to address the issue as a whole. Combining technologies and hybridizing storage systems to adapt to a multifaceted energy future is the more viable option. This paper discusses one such hybrid system, in which electrochemical energy storage is combined with renewable hydrogen production, delivering a dual platform for energy storage as an electrochemical and chemical medium.

Introduction

With the rapid development of wind and photovoltaic energy technologies in Europe and other parts of the globe, storing an excess supply of electricity is becoming an increasingly prominent issue. Due to their discontinuous and unpredictable nature, they cannot be used on a large-scale to feed the distribution grid alone, requiring mediating platforms to store the energy and release it as needed. Large-scale energy storage systems such as hydroelectric power stations are most often used, but they are geographically restricted. Compressed air (CAES) and liquid air are other promising strategies in

addressing the challenge of large scale energy storage,^{1,2} though round-trip efficiency can be at best 50%.^{1,3} Alternatively, electrochemical and hydrogen energy storage may provide a medium-to-large scale means of regulating the grid.

Electrochemical energy storage, *i.e.* batteries and accumulators are efficient and scalable means of storing energy presently.⁴ Although effective, simple and well understood, battery technology has been predominantly applied to small portable systems and somewhat larger applications in transportation. Scaling-up the power of these conventional batteries is not convenient, and presently only Li-ion and sodium–sulfur batteries are viable means of attaining high energy density batteries. Yet, large-scale energy storage and distribution structures need not be portable, thus with respect to static electrochemical systems, redox flow batteries (RFBs) are especially well designed for renewable energy storage.⁵

Energy storage using RFBs has long been studied,⁶ with two types of flow batteries having been successfully commercialized to-date: zinc–bromine⁷ and all-vanadium RFBs.⁸ All-vanadium RFBs, using V(III)/V(II) and V(V)/V(IV) redox couples, were

^aEcole Polytechnique Fédérale de Lausanne, EPFL-SB-ISIC-LEPA, Station 6, CH-1015 Lausanne, Switzerland. E-mail: hubert.girault@epfl.ch

^bEcole Polytechnique Fédérale de Lausanne, EPFL-SB-ISIC-LSCI, BCH 3305CH-1015 Lausanne, Switzerland

† Electronic supplementary information (ESI) available: Charging and discharging curves, cyclic voltammetry, UV-vis spectra of V(II) and V(III), a picture of the cell, and details on the kinetics measurement and calculations. See DOI: 10.1039/c4ee00098f

proposed by Skyllas-Kazacos *et al.* in 1986,⁹ and are now widely tested globally for the storage of renewable energy. A number of countries are integrating MW-scale RFB systems into the power grid, including the USA, Japan, Australia and Germany.¹⁰ Thus, as stand-alone energy storage systems, RFBs are a commercially available and established technology.

The advantages of using RFBs as large-scale energy storage systems are numerous. They are very flexible as storage capacity and output power are independent: capacity scales with the concentration and redox species and the volume of electrolyte, whereas the stack configuration and the number of cells control the output power. RFBs are also highly responsive with millisecond response time to load or charge, have a long lifetime of over 10 years of continuous charge/discharge cycling, and they are not affected by micro-cycles, *i.e.* incomplete charge and discharge cycles.^{10,11} Furthermore, they are of comparatively low-cost with respect to installation and maintenance, comprise relatively abundant and environmentally considerate materials and are emission free. The main drawbacks of RFBs are their relatively low energy density leading to high investment costs to achieve medium-to-large scale energy storage. Although the electrolyte volume can be increased, it remains that, once the electrolytes are charged, the battery can no longer store surplus energy until the electrolytes have been discharged to some extent through a load.

Hydrogen has long been considered a means of storing renewable energy. Theoretically hydrogen is an excellent energy carrier,¹² but to reap its benefits and transition smoothly into a functioning hydrogen economy, it must be produced, distributed and consumed efficiently and at low cost. Furthermore, it must be generated *via* clean and sustainable means, unlike the classical reforming of natural gas or coal. Converting renewable power to hydrogen gas is possible using centralised large-scale electrolyzers, in which electrical energy is converted into chemical energy (hydrogen bond) by water electrolysis. Two major types of electrolyser are the alkaline and the proton-exchange-membrane (PEM) electrolyzers.

Alkaline electrolyzers represent an established and durable system for producing H₂ in very large quantities, yet they are not ideally suited to intermittent electrolysis due to degradation of the nickel electrodes.¹³ Furthermore the possibility of H₂ and O₂ recombination within the stack,¹⁴ and the formation of bubbles at high current densities, leading to an inhomogeneous current distribution at the electrode surface are prompting alternative technologies to be sought.¹⁵ The efficiency of such systems is also mediocre, typically 50–60% for low temperature alkaline electrolyzers at 100–300 A cm⁻² and their durability is limited due to the caustic media employed.¹⁵ PEM electrolyzers are a much newer technology but are rapidly growing in interest and in size, with the conventionally small systems now being scaled-up to large, static electrolyzers.¹⁴ Presently, high installation and operating costs, predominantly due to the precious metal catalysts in the stack, prevent PEM electro-generated hydrogen from being a viable economic commodity and wide spread energy carrier.

Separating water splitting reactions from the electrochemical processes will provide a means to avoid H₂ and O₂

recombination and electrode degradation. The temporal and spatial decoupling of the oxygen and hydrogen evolution reactions using a polyoxometalate mediator were recently reported by Symes and Cronin.¹⁶ In the system presented herein, the catalysed water splitting reactions occur in separate circuits, in parallel with the RFB central circuit. Indirect water electrolysis is achieved over two catalytic beds, using the charged redox species of a conventional V–Ce RFB as the electron donor and acceptor for the hydrogen or oxygen evolution reactions. The proposed dual circuit system (Fig. 1) has the advantage of providing a secondary platform to store surplus energy beyond the capacity of the charged electrolytes, in the form of hydrogen. It is therefore a complementary technology allowing renewable electricity that would otherwise be lost when the RFB is at full capacity. Furthermore, the catalytic reactions occur independently of the electrode processes providing the opportunity to use low-cost, non-precious catalysts to obtain the hydrogen.

Results and discussion

V–Ce redox flow battery

All-vanadium RFBs have undergone extensive studies regarding thermodynamics, kinetics, cell design and stability.^{10,11,17} The cathodic redox couple, V(III)/V(II), has a standard potential of -0.26 V *vs.* SHE. It is stable under strongly acidic conditions, but is hydrolysed and precipitates at pH values higher than 2.5.¹⁸ The high solubility of V(III) and V(II) under acidic conditions allows for concentrations of up to 5 M in sulfuric acid.¹⁹ The reduction and oxidation potentials for the V(III)/V(II) redox couple were determined on polymer rod graphite electrodes *via* cyclic voltammetry of V(III) in sulfuric acid (Fig. S1, ESI†). The cyclic voltammogram corresponds well to the literature in which it has been reported that this redox couple has reasonably fast kinetics on carbon or graphite felt electrodes under various acidic conditions.^{20–23} On the graphite polymer rod in

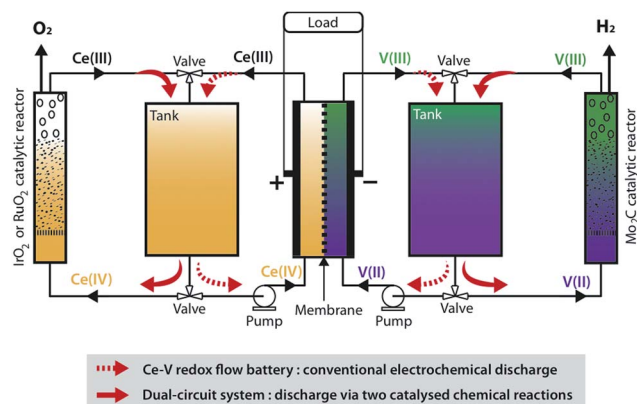


Fig. 1 The principle of indirect water electrolysis as an alternative discharge process for a V–Ce RFB. Once in the charged state (V(II) and Ce(IV)) both electrolytes may be directed in an external catalytic bed to be chemically regenerated, and then return to the RFB. The catalysed chemical reactions taking place in the catalytic beds allow the generation of hydrogen from the catholyte (V(II)) and oxygen from the anolyte (Ce(IV)).

particular, the vanadium resulted in quite reversible behaviour, with a peak separation of 67 mV and an $E_{1/2} = -0.3$ V vs. SHE at a scan rate of 20 mV s⁻¹. The graphite felt cyclic voltammograms were less defined, due to saturation of the porous material, nonetheless, reduction and oxidation peaks were evident in the region of -0.25 V vs. SHE (not shown).

The redox couple Ce(IV)/Ce(III) is largely used for redox titration, and the Ce(IV) species as an oxidative reagent in organic chemistry.²⁴ In the field of energy storage it has been employed in zinc–cerium RFBs,^{25,26} but relatively few studies have regarded V–Ce RFBs.^{25,27–30} The cerium standard potential depends on the nature of the cerium complex, *i.e.* on its coordination shell, which in turn is related to the nature of the acid and the initial cerium salt. It ranges from 1.28 V in 1 M hydrochloric acid to 1.70 V in 1 M perchloric acid.²⁴ Methanesulfonic acid (MSA) may also be used as a supporting electrolyte, either alone, or mixed with sulfuric or nitric acid. MSA is of interest due to its properties of being a “green” solvent and incurring reduced corrosion of electrode materials. It can also significantly increase the solubility of both Ce(III) and Ce(IV) ions.^{25,29} The Ce(IV)/Ce(III) oxidation and reduction potentials in MSA were reported to be 1.65 V and 1.05 V vs. SHE on a platinum electrode, displaying quasi-reversible behaviour.²⁵ In a 1 : 1 mixed MSA/H₂SO₄ solution however, the Ce(IV)/Ce(III) couple becomes considerably more reversible with a peak potential difference of just 103 mV reported by Xie *et al.*²⁹ Finally, sulfamic acid has also been studied in which quasi-reversible behaviour was observed and the redox potential was 1.52 V vs. SHE.³⁰

Sulfuric acid, nitric acid and MSA were studied as the common acidic media in the V–Ce RFB due to the variation in redox potentials expected. The addition of MSA to both nitric and sulfuric acids was also evaluated. Cyclic voltammetry was conducted on platinum and graphite electrodes, with a pre-treatment procedure applied to the platinum as outlined in previous literature.³¹ A comparison between cyclic voltammograms of Ce(IV) in 1 : 1 H₂SO₄ : MSA and 1 : 1 HNO₃ : MSA acid mixtures on the graphite polymer rod electrode is shown in Fig. S2 (ESI†). Both media resulted in quasi-reversible behaviour, and half-wave potentials of *ca.* 1.48 V vs. SHE for the H₂SO₄ mixture, and 1.61 V vs. SHE for the HNO₃ mixture were obtained. Although nitric acid resulted in a more reversible voltammetric performance, its potential use in the RFB is limited due to the cross-contamination of nitrate anions through the membrane resulting in the formation of lower nitrous oxides and the self-discharge of vanadium species. Furthermore, nitric acid requires a much more oxidative potential at the anode and also corrodes the anode electrode at an appreciable rate.

The anodic and cathodic redox couples were selected based on their ability to oxidize water and reduce protons under acidic conditions. The redox potential of the V(III)/V(II) couple renders the V(II) species highly suitable for electron donation in the hydrogen evolution reaction (HER), yet to our knowledge, the use of V(II) in this capacity has only been studied briefly in the early 1980s.^{32,33} In these publications, Parmon *et al.* used the V(II) as a reductant alongside a rhodium polyamine complex as

the HER catalyst. In the same vein Ce(IV) has frequently been used for testing water oxidation catalysts in low pH.^{34–36} Note that although both V(II) and Ce(IV) are thermodynamically capable of driving water splitting reactions, they are kinetically incapable, and only proceed in the presence of a catalyst.

In sulfuric acid, the V–Ce RFB thermodynamic cell potential is 1.7 V, which is much higher than the all-vanadium battery (1.26 V). However, only a few studies on the V–Ce RFB have been reported,^{25,27–30} and opinion of the system is somewhat divided. In order to test the feasibility of this battery for the present application, we designed and built a single-celled V–Ce RFB. Pre-treated graphite felt electrodes were used, with 100 mM Ce(III) sulfate and 100 mM V(IV) sulfate (converted to V(III)) in 1 M H₂SO₄, attaining the mean charging and discharging cell potentials of 2.5 V and 0.7 V (at 60 mA cm⁻²). The charging and discharging curves shown in Fig. S3 (ESI†) were measured under galvanostatic conditions and controlled by a galvanostat–potentiostat. The charging proceeded over 1 h and 10 min, at 60 mA cm⁻², and the discharging process was similar in length. Charging and discharging coulombic efficiencies were very high at 94% and 96%. Neither oxygen or hydrogen evolution was observed up to current densities of 80 mA cm⁻², except at the very end of the galvanostatic charging and discharging processes. The difference between charging and discharging cell potentials is due to a combination of ohmic drop and sluggish kinetics. The most dominant sources of internal resistance stem from the central Nafion membrane and the graphite felt electrodes imparting some resistance due to poor conductivity. The electrodes were improved to some extent by heat treatment, but were not thoroughly optimised. Furthermore, the quasi reversibility of both redox couples employed also decreases the voltage efficiency of the battery, especially on the Ce(IV)/Ce(III) side (Fig. S2, ESI†).

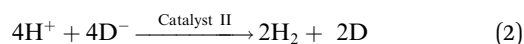
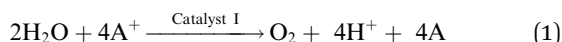
Multi-cyclic experiments indicated that the anode slightly degraded, as small black particles were visible in the cerium anolyte at high cell potential. Furthermore vanadium cations were found to be crossing the Nafion membrane, evident in the blue tinge of the Ce(III) solutions that were initially transparent. However, this only clearly occurred when the V–Ce RFB was under deep discharge and charge conditions, *i.e.* when the mediators were almost or totally converted.

A number of impeding limitations stem from the use of the cerium mediator in the system, specifically the degradation of the carbon-based electrode due to the high oxidative power of Ce(IV) and its requirement for a high anodic potential, the low solubility of Ce(III) and Ce(IV) compounds, and the difficult chemistry of Ce(III) and Ce(IV) ions, which form complex precipitates, and are very sensitive to the nature and pH of the solution. A number of these problems may be avoided however by using an alternative anode to carbon (*e.g.* boron doped diamond or titania), introducing additives such as MSA to improve solubility, and gaining further understanding of the cerium chemistry with respect to the acidic medium. Optimisation of the V–Ce RFB was not the main goal of this project and has been undertaken by other researchers.^{25,27,37} Nonetheless, the V–Ce RFB is highly suited to demonstrate indirect water splitting, as in the present system, the intended discharge is not electrochemical, but chemical.

Indirect water electrolysis

Conventionally, RFBs retain their charged redox states until connecting to an electrical load to discharge. Alternatively, both initial redox species ($V(III)$ and $Ce(III)$) may be regenerated through two separate catalysed chemical reactions, generating H_2 and O_2 in the process. In the present system, the electrolyte containing $Ce(IV)$ is passed through a secondary circuit, consisting of a catalytic bed composed of RuO_2 or IrO_2 nanoparticles (generation of O_2 , eqn (1)), whereas the electrolyte containing $V(II)$ is flowed through a second external catalytic bed, containing Mo_2C catalytic particles (generation of H_2 , eqn (2)), as depicted in Fig. 1. Both electrolytes then return to the central V–Ce RFB and the charging process is repeated. This novel system has been patented.³⁸

A particular advantage of chemically discharging the V–Ce RFB electrolytes is that a suitable design of the catalytic bed could allow the discharge to proceed considerably faster compared to conventional electrochemical discharge. This means that during peak energy production the chemical discharge allows more energy storage per unit time, therefore this system has a higher energy density than a conventional RFB. Chemical discharge could even take place at the same time as electrochemical charging if the configuration of the system is modified. The process of indirect water electrolysis is thus an alternative way of discharging the V–Ce RFB, providing a higher energy storage capacity than conventional RFBs in the form of hydrogen without considerably higher initial investment costs. The proton balance is respected if we consider two cycles and the OER and HER eqn (1) and (2) below, where A is the electron acceptor and D is the electron donor.



Although proton consumption and production will occur in the catalytic chambers, it is relative to the concentration of charged redox species. As the proton concentration is an order of magnitude higher in our lab-scale system the pH of the system will remain strongly acidic. The protons produced during water oxidation in the anolyte during the first cycle return to the V–Ce RFB, where they can pass through the proton-exchange membrane during the charging process of the second cycle and finally be reduced at the Mo_2C catalytic bed. Thus the battery need only be supplemented with water in stoichiometric quantities to the H_2 and O_2 generated.

Catalytic chambers were designed in glass tubes containing microporous fritted glass to filter the electrolyte solutions and prevent the catalytic particles from entering the main battery circuit. The electrolyte descended upon a catalytic bed following diversion from the RFB using a simple 3-way valve, returning to the electrolyte reservoir following chemical discharge. Two stills show hydrogen evolution and oxygen evolution in Fig. 2. In practice the produced hydrogen and oxygen gases may be retained in storage tanks leading from the catalytic chambers. Though atmospheric pressure and room temperature

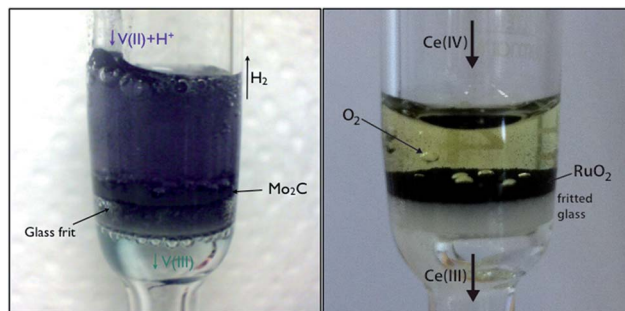


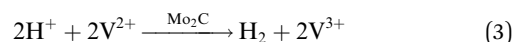
Fig. 2 Photographs of the catalytic reactions. Left: hydrogen evolution from an acidic $V(II)$ solution on a Mo_2C catalytic bed. Right: water oxidation to oxygen from an acidic $Ce(IV)$ solution on a RuO_2 catalytic bed. Hydrogen and oxygen bubbles are clearly visible.

conditions were used, a heat exchanger and a compressor could allow higher-pressure hydrogen to be stored.

The overall energy efficiency of this system, *i.e.* the ratio between the energy “contained” in the produced hydrogen and the electrical energy required to fully charge the V–Ce RFB is *ca.* 50%, considering a 60 mA cm^{-2} charging current density, 2 cm^2 electrodes, a 70 min charge time, the lower heating value for hydrogen (241 kJ mol^{-1}) and assuming a HER yield of 100% (see ESI† for a detailed calculation). The maximum thermodynamic efficiency possible from this reaction is 73%, with the 23% loss observed in the experimental lab-scale reaction is due to the battery charging performance. The difference between theoretical and experimental values may be attributed to the low voltage efficiency observed during the charge of the battery. Further optimisation of the V–Ce RFB is required in order to improve the overall efficiency of the system, particularly those of the electrodes and membrane. However, assuming the generation of hydrogen would be a means of storing surplus electricity (*i.e.* it would be lost if not stored), the overall efficiency of the system is not the most relevant criteria for future applications.

The hydrogen evolution reaction

The use of molybdenum-based electrocatalysts for the proton reduction reaction in acidic solutions has been revisited in recent years. Initially MoS_2 was recognised and successfully used in the HER,^{39–41} but very recently Mo_2C has shown an even better capability and stability.^{42–44} When integrated into an electrode, these materials display an overpotential of 150 mV for hydrogen evolution (at 10 mA cm^{-2}), and relatively long-term stability.⁴³ In the present system, the catalyst (in the form of micro-particles) is used as a heterogeneous catalyst in a fixed bed configuration, and $V(II)$ ions play the role of electron donors. The overall reaction, a redox reaction between $V(II)$ and protons, is given by eqn (3).



The global parameters of this catalytic hydrogen evolution reaction were determined by means of UV-vis spectroscopy. The solutions of 1 M sulfuric acid and 40 mM $V(II)$ were prepared in

the V–Ce RFB. The catalyst (1 ± 0.05 mg) was dispersed in 2 mL of the solution by stirring, and UV-vis spectra of the solution were measured continuously as a function of time between 480 and 1000 nm. In this spectral range the violet electron donor V(II) displays two absorption peaks with maxima at 850 nm and 570 nm, and turns to green V(III) upon oxidation, exhibiting a single absorption peak with a maximum at 600 nm. To monitor the reaction the second V(II) absorption peak (850 nm) was followed due to the overlap of the V(III) and first V(II) peaks (Fig. S4, ESI†).

The first three minutes of the reaction were considered to determine the reaction order. The rate of reaction (3), ν , was found to be first order with respect to the V(II) concentration in 1 M sulfuric acid solutions, and in the presence of 1 mg of Mo₂C. Under such conditions, the apparent rate constant k_{app} for this reaction was determined to be $k_{\text{app}} = 5.9 \times 10^{-3} \pm 0.2 \times 10^{-3} \text{ s}^{-1}$. Detailed calculations are given in the ESI.† Further measurements showed that the rate of reaction also varied with the amount of catalyst and proton concentration (pH value), indicating that these species are also implicated in the rate-limiting step of the reaction mechanism.

In order to detect possible by-products or side reactions, a batch of samples containing various V(II) concentrations, with an identical amount of dispersed catalyst were tested in septum-sealed glass vials. The reactions were driven to completion by mixing the solutions for at least two hours. The amount of hydrogen contained in the headspace of each glass vial was measured by gas chromatography (GC), and compared to a calibration curve. The reaction yield was $96 \pm 4\%$ as shown in Fig. 3, showing no significant side reaction occurred and nearly maximum conversion efficiency was achieved.

The water oxidation reaction

Water oxidation is a notoriously difficult reaction due to kinetic limitations related to high-energy barriers for the formation of

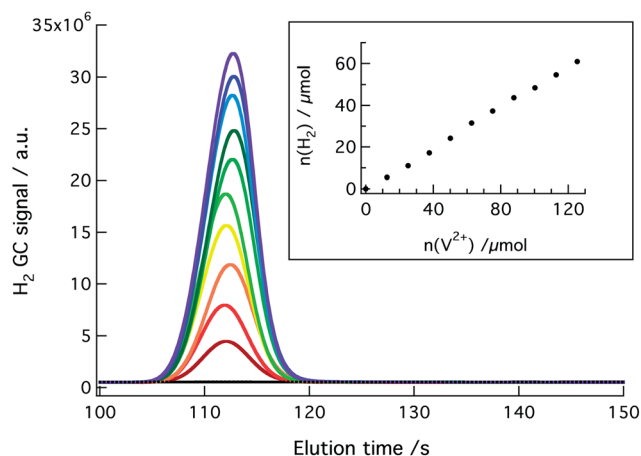
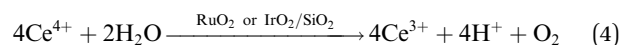


Fig. 3 Hydrogen GC signals for 2 mL solutions containing various concentrations of V(II) (0, 10, 20, 40, 50, 60, 80, 100, 150, and 200 mM) in 1 M H₂SO₄ and 1 mg of Mo₂C. The inset shows the amount of hydrogen produced for the corresponding initial amount of V(II) in the solution.

intermediates and transition states.^{45,46} It is especially difficult under acidic conditions, as most studied catalysts operate in neutral or alkaline solutions. Catalysed chemical water oxidation under strongly acidic conditions was therefore studied in detail in order to determine its feasibility and efficiency, using IrO₂ nanoparticles or RuO₂ microparticles as the catalyst and Ce(IV) as the electron donor.

Under 1 M strong acid (H₂SO₄, HNO₃, MSA or acid mixtures) conditions the pH of the solution is about 0, therefore the standard potential for water oxidation into oxygen is 1.23 V vs. SHE. It was first observed that Ce(IV) sulfate in sulfuric acid, with a standard potential of 1.44 V vs. SHE, was not able to oxidise water in the presence of supported IrO₂, however with heat pre-treated RuO₂ microparticles the reaction did proceed. This indicated that the overpotential imparted by the catalysts was crucial. The difference in the catalytic potential of different water oxidation catalysts is recognised in the literature, with an OER catalytic potential of 1.44 V (the same as Ce(IV)/Ce(III) in 1 M H₂SO₄) attributed to IrO₂ and a catalytic potential of 1.36 V (ref. 47–49) to RuO₂.

As previously mentioned, the Ce(IV)/Ce(III) standard potential depends on the ligands attached to the cerium centre, and was reported to vary between 1.28 V and about 1.7 V vs. SHE.²⁴ An investigation of various acids, mixtures of acids, and cerium salts, in terms of electrochemical reversibility on graphite electrodes and efficiency as electron acceptor in the OER, was conducted. Pre-studies showed that in nitric acid, MSA, and mixtures of both, the IrO₂ catalysed OER (eqn (4)) was possible using cerium ammonium nitrate (CAN) as the initial salt. More details are given in the ESI (Fig. S5†).



The kinetics of the OER using Ce(IV) sulfate generated in 1 M H₂SO₄ in the V–Ce RFB were studied using the pre-treated RuO₂ catalyst. RuO₂ is the most widely studied water oxidation catalyst. The catalyst used here was commercial, hydrated RuO₂ that was heated in air at 150 °C overnight, as per the procedure outlined by Mills and Russell.⁵⁰ Anhydrous and as-bought hydrous RuO₂ were also studied, and were entirely inactive towards water oxidation. The pre-treated material was highly active however, and seemingly fully converted the Ce(IV) to Ce(III).

In Fig. S6 (ESI†), the generation of oxygen, and the corresponding consumption of Ce(IV) as a function of the amount of catalyst added to the shake flask is shown. Based on three identical measurements (0.5 mg RuO₂ + 0 to 50 mM Ce(IV) sulfate in 1 M H₂SO₄, high mixing rate, under N₂ atmosphere), the reaction order in the first three minutes for reaction (4) was observed to be unity with respect to Ce(IV) concentration. An apparent rate constant of $k_{\text{app}} = 3.08 \times 10^{-4} \pm 0.34 \times 10^{-4} \text{ s}^{-1}$ was found for the same measurements. Detailed calculations are given in the ESI.† The yield of the reaction was measured by varying the concentration of Ce(IV), keeping all the other experimental conditions constant, and by driving the reaction to completion. The amount of oxygen produced was then measured by GC and compared to the amount of Ce(IV) initially

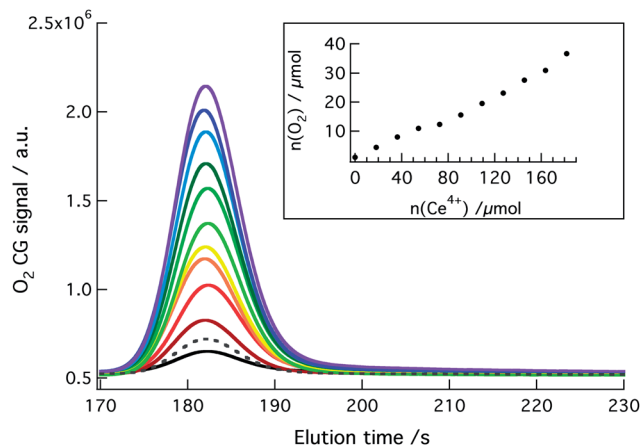
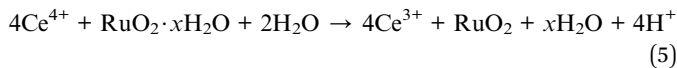


Fig. 4 Oxygen GC signals for 2 mL solutions of Ce(IV) (0, 10, 20, 30, 40, 50, 60, 70, 80, 90 and 100 mM) in 1 M H₂SO₄ and 0.5 mg of hydrated RuO₂. The dashed line is for 100 mM of Ce(IV), without catalyst. Reaction time was at least 2 hours. The inset displays the amount of oxygen which was produced for the corresponding initial amount of Ce(IV) in the solution.

present in the solution (Fig. 4). The mean conversion over 10 samples was $78 \pm 8\%$, which indicates the presence of side reactions. Mills and Russell⁵⁰ suggested that RuO₂, when hydrated, is corroded by the Ce(IV) cations according to eqn (5). Even if the catalyst is expected to be only partially hydrated,⁵⁰ Ce(IV) ions may have been consumed by this oxidation reaction. This was also supported by the observation that the catalyst was becoming less active with reaction time, and when reused several times.



Thermodynamics vs. kinetics

The key concept central to this paper is the interplay of theoretical thermodynamic water electrolysis and the kinetically feasible process. As illustrated in Fig. 5 there is a large difference between the thermodynamic potentials for water electrolysis (HER 0 V, OER 1.23 V vs. SHE) and the generally observed potentials *i.e.* the kinetic overpotentials. Generally, by employing catalysts these overpotentials can be decreased and water electrolysis may occur at potentials closer to the theoretical, however, for water oxidation in particular, the intrinsic kinetic barriers owing to the multiproton and multielectron reaction remain. Electrochemical water oxidation is rarely achieved with less than 200 mV overpotential, with commercial electrolyzers usually operating at a cell potential of about 2 V.

In the system proposed here the RFB redox reactions occur at potentials in between the thermodynamic lower limit and the kinetic upper limit. When little overpotential is required to drive the reaction, as in the case for the V(III)/V(II) reaction, a solution of electron donor may be readily produced with high coulombic efficiency. In a chemical reaction in the presence of a catalyst the donor can effectively donate those electrons to produce hydrogen and V(III), at a rate that far exceeds

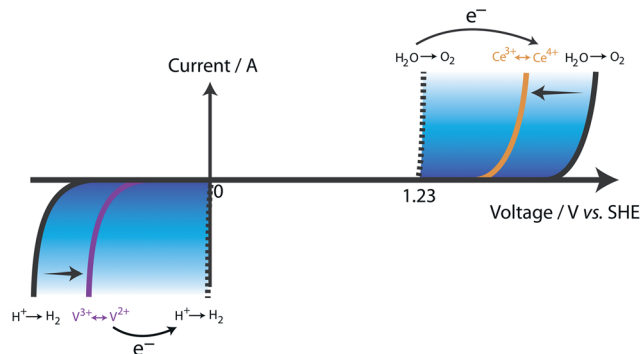


Fig. 5 Principle of indirect water electrolysis. On this scheme, the thermodynamic reduction potential for both reactions of water electrolysis, hydrogen evolution and oxygen evolution (dashed lines) are compared to the actual electrode potential applied to observe these reactions on graphite electrodes (black lines) and the intermediate redox potentials of suitable redox mediators *e.g.* V(III)/V(II) and Ce(IV)/Ce(III).

electrochemical transfer and with stoichiometric control and very high efficiency. Although cerium oxidation is less kinetically favourable, depending greatly on the acid medium, it too can be converted at a potential intermediate of the thermodynamic and kinetic limits. Optimisation and careful selection of the RFB electrolytes may lead to electrolytic processes that are more favourable than direct electrolysis at an electrode. The focus of the dual-circuit RFB is the generation of hydrogen at the cathodic catalytic bed and not the process of oxygen evolution. As a proof of concept indirect water electrolysis presented here completes the modified RFB circuit, allowing for the chemical discharge of both charged electrolytes. However, the potential for numerous alternative anolyte discharge processes is available, including chlorine evolution, the chemical oxidation of organic pollutants, hydrazine oxidation (to N₂ and protons) and sulfur dioxide oxidation to sulfuric acid. Furthermore, the system is not limited to using cerium in the anolyte, as an all-vanadium RFB that can be chemically discharged in some similar manner could also be considered. The concept here is indirect electrolysis, in which hydrogen is evolved effectively and efficiently from a charged vanadium catholyte, and oxygen from the charged cerium anolyte.

Conclusions

An alternative indirect water electrolysis process, based on a dual-circuit V–Ce RFB has been presented. Electrical energy is used to electrochemically reduce and oxidise vanadium and cerium species respectively during the conventional charging of the RFB. In the charged state, the positive redox mediator is used as an electron acceptor in catalysed water oxidation, whereas the negative redox mediator is used as an electron donor in catalysed proton reduction. This chemical discharge takes place in two separate catalytic beds forming a secondary circuit that is appended to the central V–Ce RFB. The system is thus capable of storing electrical energy in the form of charged redox species, or in the hydrogen–hydrogen bond, the latter

reproducing the discharged species for reuse in the battery during periods of peak electricity production.

For an all sulfuric acid battery, the coulombic charging efficiency of the battery is 94% (at 60 mA cm⁻²). Hydrogen was generated from V(II) using an abundant and low cost Mo₂C catalyst and achieved a production yield of 96 ± 4%. Water oxidation was achieved over IrO₂ and RuO₂ nanoparticles from positive electrolytes comprising Ce(IV) in various acid solutions. A 78 ± 8% O₂ yield was obtained in 1 M H₂SO₄ and a partially hydrated RuO₂ catalyst.

This system is unique in the field of energy storage, merging two highly pursued technologies: renewable electrochemical energy storage and renewable power-to-gas. The novel technique allows surplus electricity to be stored as hydrogen beyond the limited energy density of the RFB electrolytes, with rapid discharge of the electrolytes also possible to provide an immediate sink for excess electricity. As water oxidation is not of commercial interest, alternative discharge reactions for the anolyte must be investigated. With commercial all-vanadium RFBs the chemical discharge of the positive V(V) species may also be envisaged, such as reduction by hydrazine to produce protons and N₂, SO₂ oxidation to produce H₂SO₄, or the oxidation of wastewater pollutants. Further investigation into optimising the anolyte discharge and to further characterise the catalytic reactions are in progress.

Experimental

Redox flow battery

The anodic solutions prepared were 0.1 M Ce(III) from either the cerium(III) sulfate hydrate (Aldrich) or the ammonium cerium(III) nitrate (CAN) (ACS 99%, Acros Organics) in 50 mL of 1 M strong acid (H₂SO₄, HNO₃, methanesulfonic acid, or mixture of acids with a total concentration of 1 M). Similarly, a cathodic solution of 0.1 M vanadium was prepared from VOSO₄ in 1 M H₂SO₄. The acid solutions were prepared by diluting concentrated nitric acid (65%, Fluka), concentrated sulfuric acid (ISO 95–97%, Merck) or methanesulfonic acid (methanesulfonic acid solution, 70 wt %, Sigma-Aldrich) in ultrapure water (18.2 MΩ cm). Solutions were deoxygenated in their RFB storage tanks for at least 20 minutes with nitrogen (N₂ 45, Carbagas) before being circulated through the battery at a constant flow rate of 50 mL min⁻¹. A continuous flow of nitrogen was maintained in both storage tanks during the charging and discharging processes.

The electrochemical cell was built in-house using custom designed Teflon pieces. A full description and corresponding figure of the system is given in the ESI (Fig. S7†). In brief, the cell consisted of two Teflon external parts, two 3 mm thick Viton seals, and a pre-treated Nafion® N117 ion-exchange membrane (Ion Power Inc.). Each half-cell contained a boron doped diamond (W260, Adamantec) current collector plate mounted on stainless steel, which was connected to the external electrical circuit on the backside through a steel rod. The electrodes were graphite felt (Sigratherm GFD5 EA, SGL Group) of dimension 0.5 × 0.5 × 4 cm. They were pre-treated by heating in an oven at 400 °C for 4 hours in air. A peristaltic pump (Reglo Dig. MS,

Ismatec) was used to drive both electrolytes through the Teflon tube circuit. An Autolab (PGSTAT128N, Metrohm Autolab B.V.) was used to measure the galvanostatic charge and discharge of the RFB and two multimeters (UNI-T UT71E, Uni-Trend Technology Limited, China) were used to monitor the discharge when an external resistance was used.

The total concentration of vanadium, respectively cerium was measured by ICP-OES analysis performed with an Optima 2000 spectrometer (Perkin-Elmer). A standard TraceCERT (1 g L⁻¹, Aldrich) was used for vanadium calibration, whereas a standard solution of cerium(IV) ammonium nitrate (Aldrich) was prepared from a dried salt (heated at 85 °C overnight) and used for cerium calibration. The concentration of Ce(IV) in the solution was also measured by indirect iodine titration. A known volume of the analysed solution was diluted in 10 mL of a 1 M sulfuric acid solution and an excess of potassium iodide (Fluka) was added. The iodine produced was titrated with sodium thiosulfate (anhydrous, 99%, Alfa Aesar), and a small amount of potato starch (Fluka).

Catalytic beds

The catalytic beds were prepared from glass funnel containing a fritted glass filter (Por. 4, 11 to 16 μm). Catalytic powder was placed on top of the fritted glass, and the charged RFB solution was diverted using a 3-way valve to flow through the catalytic layer and the filter. The flow rate of the electrolytes through the catalytic beds was about 1 mL min⁻¹. Such a low value was required due to the flow resistance exhibited by the fritted glass and the catalytic bed. After the reaction, the flow of discharged solution was redirected to the appropriate storage tank in the RFB.

Catalyst preparation

Mo₂C (325 mesh, Aldrich) catalyst was used as received for the kinetic measurements. Structural information on the catalyst have been reported elsewhere.⁴³ The catalytic bed was first treated with a 1 M H₂SO₄ solution, in order to remove the particles small enough to pass through the fritted glass, to prevent any from entering the redox flow battery.

Hydrated RuO₂ (ruthenium(IV) hydrate, Fluka) was pre-treated in accordance with studies by Mills and Russell.⁵⁰ A portion of the compound was partially dehydrated in air at 150 °C for at least 6 hours. The catalyst was then used directly to form a catalytic bed in a Por. 4 fritted glass tube. The synthesis procedure for IrO₂ nanoparticles immobilised on SiO₂ is detailed in the ESI.†

UV-vis measurements

All UV-vis measurements were conducted inside a glovebox (maximum oxygen content: 3 ppm). Calibration curves for V(II) and V(III) were established between 0 and 100 mM in 1 M sulfuric acid solutions. The kinetics were analysed using a spectrophotometer (CHEM2000 UV-vis, Ocean Optics Switzerland) placed on a magnetic plate to allow constant agitation of the sample. The blank was always the corresponding acid solution. For the kinetic measurements, the UV-vis spectra as a

function of time were recorded automatically with the software OOIBase32 (Version 1.0.3.0, Ocean Optics).

Gas quantification

A gas chromatograph (AutoSystem, Perkin Elmer) based on an injection loop, a molecular sieve packed column ($12' \times 1/8''$ SS Column, Molecular Sieves 5A 100/80, Perkin Elmer), and a TCD detector were used for the quantification of oxygen and hydrogen. To proceed to the measurement, the headspace of the septum-sealed flask was sampled with a gastight lock-in syringe, and then injected into the injection loop of the gas chromatograph. The obtained data were compared to a calibration curve.

To determine the water oxidation kinetic parameters reactions were conducted using a fluorimetric oxygen sensor (NeoFox, FOXY probe, Ocean Optics) in 4 mL septum-sealed flasks, under a nitrogen atmosphere. All solutions were deoxygenated and the catalyst powder added to the flask (in the glovebox) before the setup of the flask in the deoxygenated NeoFox compartment. The reactive solution (2 mL) was added through the septum with a syringe and the oxygen detector measured the amount of oxygen in the headspace of the flask as a function of time. Data were recorded automatically every 500 ms.

Acknowledgements

The present project is supported by EOS Holding SA (Switzerland) for LEPA and by the European Research Council for LSCI (starting grant no. 257096). We thank Micheál Scanlon and Jonnathan Hidalgo for their help regarding the IrO₂ catalyst.

References

- H. Chen, T. N. Cong, W. Yang, C. Tan, Y. Li and Y. Ding, *Prog. Nat. Sci.*, 2009, **19**, 291–312.
- H. Lund and G. Salgi, *Energy Convers. Manage.*, 2009, **50**, 1172–1179.
- H. Ibrahim, A. Ilinca and J. Perron, *Renewable Sustainable Energy Rev.*, 2008, **12**, 1221–1250.
- B. Dunn, H. Kamath and J. M. Tarascon, *Science*, 2011, **334**, 928–935.
- T. Nguyen and R. F. Savinell, *Electrochem. Soc. Interface*, 2010, **19**, 54–56.
- L. H. Thaller, The United States of America as represented by the Administrator of the National Aeronautics and Space Administration, *US Pat.*, 3,996,064, 1976.
- E. Kantner, Exxon Research & Engineering Co. (Florham Park, New Jersey, United States), *US Pat.*, 4,491,625, 1985.
- M. Skyllas-Kazacos, M. Rychick and R. Robins, Uniresearch Limited (Australia), *US Pat.*, 4,786,567, 1988.
- M. Skyllas-Kazacos, *J. Electrochem. Soc.*, 1986, **133**, 1057.
- A. Z. Weber, M. M. Mench, J. P. Meyers, P. N. Ross, J. T. Gostick and Q. Liu, *J. Appl. Electrochem.*, 2011, **41**, 1137–1164.
- M. Skyllas-Kazacos, M. H. Chakrabarti, S. A. Hajimolana, F. S. Mjalli and M. Saleem, *J. Electrochem. Soc.*, 2011, **158**, R55.
- A. Midilli, M. Ay, I. Dincer and M. A. Rosen, *Renewable Sustainable Energy Rev.*, 2005, **9**, 255–271.
- W. Hu, *Int. J. Hydrogen Energy*, 2000, **25**, 111–118.
- M. Carmo, D. L. Fritz, J. Mergel and D. Stolten, *Int. J. Hydrogen Energy*, 2013, **38**, 4901–4934.
- K. Zeng and D. Zhang, *Prog. Energy Combust. Sci.*, 2010, **36**, 307–326.
- M. D. Szymes and L. Cronin, *Nat. Chem.*, 2013, **5**, 403–409.
- C. Ponce-de-León, A. Frías-Ferrer, J. González-García, D. A. Szánto and F. C. Walsh, *J. Power Sources*, 2006, **160**, 716–732.
- K. Post and R. G. Robins, *Electrochim. Acta*, 1976, **21**, 401–405.
- F. Rahman and M. Skyllas-Kazacos, *J. Power Sources*, 1998, **72**, 105–110.
- C. Gao, N. Wang, S. Peng, S. Liu, Y. Lei, X. Liang, S. Zeng and H. Zi, *Electrochim. Acta*, 2013, **88**, 193–202.
- K. J. Kim, Y.-J. Kim, J.-H. Kim and M.-S. Park, *Mater. Chem. Phys.*, 2011, **131**, 547–553.
- X. Li, K. Huang, S. Liu, N. Tan and L. Chen, *Trans. Nonferrous Met. Soc. China*, 2007, **17**, 195–199.
- X. W. Wu, T. Yamamura, S. Ohta, Q. X. Zhang, F. C. Lv, C. M. Liu, K. Shirasaki, I. Satoh, T. Shikama, D. Lu and S. Q. Liu, *J. Appl. Electrochem.*, 2011, **41**, 1183–1190.
- K. A. J. Gschneidner, J.-C. G. Bünzli and V. K. Pecharsky, *Handbook on the Physics and Chemistry of Rare Earths*, Elsevier, 2006.
- P. K. Leung, C. Ponce-de-León, C. T. J. Low and F. C. Walsh, *Electrochim. Acta*, 2011, **56**, 2145–2153.
- G. Nikiforidis, L. Berlouis, D. Hall and D. Hodgson, *J. Power Sources*, 2012, **206**, 497–503.
- Y. Liu, X. Xia and H. Liu, *J. Power Sources*, 2004, **130**, 299–305.
- X. Xia, H.-T. Liu and Y. Liu, *J. Electrochem. Soc.*, 2002, **149**, A426.
- Z. Xie, F. Xiong and D. Zhou, *Energy Fuels*, 2011, **25**, 2399–2404.
- F. Xiong, D. Zhou, Z. Xie and Y. Chen, *Appl. Energy*, 2012, **99**, 291–296.
- T. H. Randle and A. T. Kuhn, *J. Chem. Soc., Faraday Trans. 1*, 1983, **79**, 1741–1756.
- E. R. Buyanova, L. G. Matvienko, A. I. Kokorin, G. L. Elizarova, V. N. Parmon and K. I. Zamaraev, *React. Kinet. Catal. Lett.*, 1981, **16**, 309–313.
- K. I. Zamaraev and V. N. Parmon, *Russ. Chem. Rev.*, 2007, **52**, 817.
- J. D. Blakemore, N. D. Schley, G. W. Olack, C. D. Incarvito, G. W. Brudvig and R. H. Crabtree, *Chem. Sci.*, 2010, **2**, 94–98.
- D. Hong, M. Murakami, Y. Yamada and S. Fukuzumi, *Energy Environ. Sci.*, 2012, **5**, 5708–5716.
- A. R. Parent, R. H. Crabtree and G. W. Brudvig, *Chem. Soc. Rev.*, 2013, **42**, 2247.
- A. Paulenova, S. E. Creager, J. D. Navratil and Y. Wei, *J. Power Sources*, 2002, **109**, 431–438.
- V. Amstutz, K. E. Toghiani, C. Comninellis and H. H. Girault, EOS Holding (Switzerland), *International Pat.*, WO 2013131838, 2013.

- 39 P. Ge, M. D. Scanlon, P. Peljo, X. Bian, H. Vubrel, A. O'Neill, J. N. Coleman, M. Cantoni, X. Hu, K. Kontturi, B. Liu and H. H. Girault, *Chem. Commun.*, 2012, **48**, 6484.
- 40 B. Hinnemann, P. G. Moses, J. Bonde, K. P. Jørgensen, J. H. Nielsen, S. Horch, I. Chorkendorff and J. K. Nørskov, *J. Am. Chem. Soc.*, 2005, **127**, 5308–5309.
- 41 V. W.-h. Lau, A. F. Masters, A. M. Bond and T. Maschmeyer, *ChemCatChem*, 2011, **3**, 1739–1742.
- 42 W. F. Chen, C. H. Wang, K. Sasaki, N. Marinkovic, W. Xu, J. T. Muckerman, Y. Zhu and R. R. Adzic, *Energy Environ. Sci.*, 2013, **6**, 943–951.
- 43 H. Vrubel and X. L. Hu, *Angew. Chem., Int. Ed.*, 2012, **51**, 12703–12706.
- 44 S. Wirth, F. Harnisch, M. Weinmann and U. Schroeder, *Appl. Catal., B*, 2012, **126**, 225–230.
- 45 F. A. Armstrong, *Philos. Trans. R. Soc., B*, 2008, **363**, 1263–1270.
- 46 M. Hara and T. E. Mallouk, *Chem. Commun.*, 2000, 1903–1904.
- 47 L. Ouattara, S. Fierro, O. Frey, M. Koudelka and C. Comninellis, *J. Appl. Electrochem.*, 2009, **39**, 1361–1367.
- 48 R. D. L. Smith, M. S. Prévot, R. D. Fagan, Z. Zhang, P. A. Sedach, M. K. J. Siu, S. Trudel and C. P. Berlinguette, *Science*, 2013, **340**, 60–63.
- 49 E. Tsuji, A. Imanishi, K.-I. Fukui and Y. Nakato, *Electrochim. Acta*, 2011, **56**, 2009–2016.
- 50 A. Mills and T. Russell, *J. Chem. Soc., Faraday Trans.*, 1991, **87**, 1245–1250.